Pergamon

Int. J. Heat Mass Transfer. Vol. 40, No. 9, pp. 2045–2053, 1997

0017–9310/97 $17.00+0.00

PII: S0017-9310(96)00280-3

An inverse geometry problem in identifying irregular boundary configurations

CHENG-HUNG HUANG and BOR-HERNG CHAO
Department of Naval Architecture and Marine Engineering, National Cheng Kung University, Tainan, Taiwan, Republic of China

(*Received* 22 *December* 1995 *and in final form* 5 *August* 1996)

Abstract—An inverse geometry heat conduction problem (shape identification problem) is solved to detect the unknown irregular boundary shape by using the boundary element method (BEM)-based inverse algorithms. They are the Levenberg–Marquardt method (L–MM) and the conjugate gradient method (CGM), respectively.

A sequence of forward steady-state heat conduction problems is solved in an effort to update the boundary geometry by minimizing a residual measuring the difference between actual and computed temperatures at the sensor's locations under the present two algorithms.

Results obtained by using both schemes to solve the inverse problems are compared based on the numerical experiments. One concludes that the conjugate gradient method is better than the Levenberg–Marquardt method since the former one: (i) needs very short computer time; (ii) does not require a very accurate initial guess of the boundary shape; and (iii) needs less number of sensors. Finally the effects of the measurement errors to the inverse solutions are discussed.

1. INTRODUCTION

The applications of inverse problems can be found in several engineering fields, such as the determination of boundary conditions [1–2], thermal properties [3–4], heat generation [5], contact resistance [6], etc. Recently, thermal imaging becomes another area of active inverse problem research and much research has been devoted to infrared scanners and their applications to nondestructive evaluation (NDE) [7–9]. The approaches taken to solve NDE problems are based on either study- or unsteady-state response of a body subjected to thermal sources.

In this paper two formulations, i.e. the Levenberg–Marquardt method [10] and the conjugate gradient method [1–3, 6] for the numerical solution to the inverse geometry problem of identifying the unknown irregular boundary configurations from external measurements (either direct or infrared type), based on a boundary element method, are considered. Such identification problems can be stated in various contexts; acoustics, elastodynamics, thermal sciences and can lead to the applications to NDE techniques and other identification problems.

The use of boundary element method is suggested by the basic nature of the inverse problem (to search an unknown domain, thus an unknown surface), because domain discretization is avoided. More specifically, the advantages gained by BEM-based algorithm is the ability to readily accommodate the changes in the unknown boundary shape as it evolves from its initial to its final shape.

The present work addresses the developments of both the Levenberg–Marquardt and conjugate gradient algorithms, for estimating unknown boundary shape. The Levenberg–Marquardt method combines the Newton's and steepest-descent methods and has the advantage of fast convergence when the unknown parameters are few. The conjugate gradient method derives basis from the perturbation principles and transforms the inverse problem to the solution of three problems, namely, the direct problem, the sensitivity problem and the adjoint problem. These two methods will be discussed in detail in the text.

2. THE DIRECT PROBLEM

To illustrate the methodology for developing expressions for use in determining unknown boundary geometry in a homogeneous medium, we consider the following two-dimensional steady-state inverse heat conduction problem. For a domain Ω, the boundary conditions at $x = 0$ and L are assumed both insulated, at $y = 0$, a constant heat flux q_0 is taken away from the boundary by cooling while the boundary condition at $y = f(x)$ maintains at a uniform temperature T_0. Figure 1 shows the geometry and the coordinates for the two-dimensional physical problem considered here. The mathematical formulation of this steady-state heat conduction problem in dimensionless form is given by:

$$\frac{\partial^2 T}{\partial x^2} + \frac{\partial^2 T}{\partial y^2} = 0 \quad \text{in } \Omega \tag{1a}$$

$$\frac{\partial T}{\partial x} = 0 \quad \text{at } x = 0 \tag{1b}$$

NOMENCLATURE

$f(x)$ unknown irregular boundary configuration
G, H geometry dependent matrix
J functional defined by equation (5)
J' gradient of functional defined by equation (18)
P direction of descent defined by equation (10b)
q heat flux density
$T(x, y)$ estimated dimensionless temperature
$\Delta T(x, y)$ sensitivity function defined by equation (11)
$Y(x, 0)$ measured temperature.

Greek symbols
β search step size
γ conjugate coefficient
Ω computational domain
Γ boundary of the computational domain
Φ Jacobian matrix
μ damping parameter
$\lambda(x, y)$ Lagrange multiplier defined by equation (16)
$\delta(\bullet)$ Dirac delta function
ω random number
ε convergence criteria
σ standard deviation of the measurement errors.

Superscripts
$\hat{}$ estimated values
n iteration index
$*$ fundamental solution.

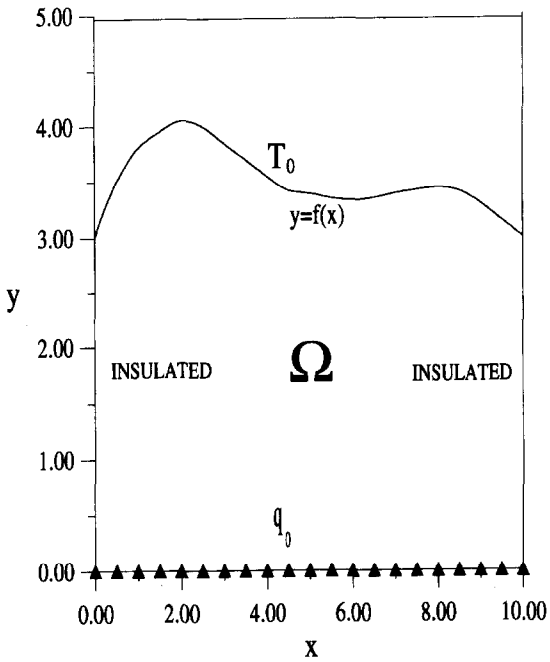

Fig. 1. Geometry and coordinates.

$$\frac{\partial T}{\partial x} = 0 \quad \text{at } x = L \tag{1c}$$

$$-\frac{\partial T}{\partial y} = q_0 \quad \text{at } y = 0 \tag{1d}$$

$$T = T_0 \quad \text{at } y = f(x). \tag{1e}$$

The above problem is solved by the following a BEM algorithm: for a constant property, steady-state heat conduction problem with a domain Ω and boundary Γ, the boundary integral equation for this problem without generation term can be derived as [11]:

$$cT_M + \int_\Gamma Tq^* \, d\Gamma = \int_\Gamma qT^* \tag{2}$$

where M = point of Γ or Ω; T = temperature; q = heat flux density; $c = 1$, if M is in Ω; $c < 1$, if M is on Γ ($c = 0.5$ if Γ is smooth at M); T^* = stationary fundamental solution; q^* = normal derivative of T^*; thus [11]

$$T^* = \frac{1}{2\pi} \ln\left(\frac{1}{r}\right) \quad \text{in two dimensions}$$

and

$$T^* = \frac{1}{4\pi r} \quad \text{in three dimensions}$$

where r = distance from M to a point of Γ.

When considering direct problems, if M is on Γ, one has with equation (2) the basic equation for potential problems. For M in Ω, the boundary integral equation which then connect internal temperatures and boundary fields are usually used for a posteriori computation.

Generally speaking, the discretization of Γ into k boundary elements allows substitution into the boundary integral equation (2) expressed for each boundary element of the algebraic linear system

$$\mathbf{CT} + \mathbf{HT} = \mathbf{Gq} \tag{3}$$

where $\mathbf{T}$ = vector of temperature boundary elements; $\mathbf{q}$ = vector of the heat flux densities; $\mathbf{H}, \mathbf{G}$ = geometry dependent matrices; $\mathbf{C}$ = diagonal matrix.

Once all unknowns are passed to the left-hand-side one can write

$$\mathbf{AX} = \mathbf{B} \tag{4}$$

where **X** is the vector of unknown Ts and qs boundary values. **B** is found by multiplying the corresponding columns by the known values of Ts or qs.

The computer program for the above stated problem is modified based on the text book by Brebbia and Dominguez [11] and the linear boundary elements are adopted for all the examples illustrated here. The direct problem considered here is concerned with the determination of the medium temperature when the boundary geometry $f(x)$ and the boundary conditions at all boundaries are known.

3. THE INVERSE PROBLEM

For the inverse problem, the boundary geometry $f(x)$ is regarded as being unknown, but everything else in equation (1) is known. In addition, temperature readings taken at some appropriate locations are considered available. Referring to Fig. 1, we assumed that m sensors installed along $y = 0$ are used to record the temperature information to identify boundary configuration $f(x)$ in the inverse calculations. Let the temperature reading taken within these sensors be denoted by $Y(x_i, 0) \equiv Y_i, i = 1$–$m$, where m represents the number of thermocouples. We note that the measured temperature Y_i contains measurement errors. Then the inverse problem can be stated as follows: by utilizing the above-mentioned measured temperature data Y_i, estimate the unknown upper boundary shape $f(x)$.

The solution of the present inverse problem is to be obtained in such a way that the following functional is minimized:

$$J[f(x)] = \sum_{i=1}^{m} [T_i - Y_i]^2 = \mathbf{U}^T\mathbf{U} \tag{5}$$

here, T_i are the estimated or computed temperatures at the measurement locations $(x_i, 0)$. These quantities are determined from the solution of the direct problem given previously by using an estimated $\hat{f}(x)$ for the exact $f(x)$. Here the hat "^" denotes the estimated quantities.

4. THE LEVENBERG–MARQUARDT METHOD FOR MINIMIZATION

If the unknown boundary shape is discretized into k linear elements, there exist $(k+1)$ discretized values of $f(x)$, say, $f(x) = \mathbf{f} = f_j = \{f_0, f_1, \ldots, f_k\}$, $j = 0$–k. Equation (5) is minimized with respect to the estimated parameters f_j to obtain

$$\frac{\partial J}{\partial f_j} = \sum_{i=1}^{m} \left[\frac{\partial T_i}{\partial f_j}\right][T_i - Y_i] = 0; \quad j = 0\text{–}k \tag{6}$$

where m should be equal to or greater than $(k+1)$, otherwise an underdetermined system of equations will be obtained and it is impossible to calculate the inverse solutions under this situation. Equation (6) is linearized by expanding $T_i(f_j)$ in Taylor series and retaining the first-order terms. Then a damping parameter μ^n is added to the resulting expression to improve convergence, leading to the Levenberg–Marquardt method [10] given by

$$(\mathbf{F} + \mu^n\mathbf{I})\,\Delta\mathbf{f} = \mathbf{D} \tag{7a}$$

where

$$\mathbf{F} = \mathbf{\Phi}^T\mathbf{\Phi} \tag{7b}$$

$$\mathbf{D} = \mathbf{\Phi}^T\mathbf{U} \tag{7c}$$

$$\Delta\mathbf{f} = \mathbf{f}^{n+1} - \mathbf{f}^n. \tag{7d}$$

Here the superscripts n and T represent the iteration index and transport matrix, respectively, **I** is the identity matrix and $\mathbf{\Phi}$ denotes the Jacobian matrix defined as

$$\mathbf{\Phi} \equiv \frac{\partial \mathbf{T}}{\partial \mathbf{f}^T}. \tag{8a}$$

The Jacobian matrix defined by equation (8a) is determined by perturbing the unknown parameters f_j one at a time and computing the resulting change in temperature from the solution of the direct problem (equation 1).

Equation (7a) is now written in a form suitable for iterative calculation as

$$\mathbf{f}^{n+1} = \mathbf{f}^n + (\mathbf{\Phi}^T\mathbf{\Phi} + \mu^n\mathbf{I})^{-1}\mathbf{\Phi}^T(\mathbf{T} - \mathbf{Y}). \tag{8b}$$

When $\mu^n = 0$, the Newton's method is obtained; as $\mu^n \to \infty$, the steepest-descent method is obtained. For fast convergence the steepest-descent method is applied first, then the value of μ^n is decreased; finally, the Newton's method is used to obtain the inverse solution. The algorithm of choosing this damping value μ^n is described in detail in [10], so they are not repeated here.

4.1. *Stopping criterion*

If the problem contains no measurement errors, the traditional check condition is specified as

$$J[\hat{f}^{n+1}(x)] < \varepsilon \tag{9a}$$

where ε is a small specified number. However, the observed temperature data may contain measurement errors. Therefore, we do not expect the functional equation (5) to be equal to zero at the final iteration step. Following the experience of the authors [1–3], we use the discrepancy principle as the stopping criterion, i.e. we assume that the temperature residuals may be approximated by

$$T_i - Y_i \approx \sigma \tag{9b}$$

where σ is the stand deviation of the measurements,

which is assumed to be a constant. Substituting equation (9b) into equation (5), the following expression is obtained for ε:

$$\varepsilon = m\sigma^2. \tag{9c}$$

Then, the stopping criterion is given by equation (9a) with ε determined from equation (9c).

4.2. *Computational procedure*

The iterative computational procedure for the solution of this inverse problem using Levenberg–Marquardt method can be summarized as follows: choose the initial guess **f** at iteration n to start the computation.

Step 1. Solve the direct problem given by equation (1) to obtain computed temperature **T**.

Step 2. Construct the Jacobian matrix in accordance with equation (8a).

Step 3. Update **f** from equation (8b).

Step 4. Check the stopping criteria given by equation (9).

5. CONJUGATE GRADIENT METHOD FOR MINIMIZATION

The following iterative process based on the conjugate gradient method [1–3, 6] is now used for the estimation of unknown boundary function $f(x)$ by minimizing the functional $J[f(x)]$

$$\hat{f}^{n+1}(x) = \hat{f}^n(x) - \beta^n P^n(x) \quad \text{for } n = 0, 1, 2, \ldots \tag{10a}$$

where β^n is the search step size in going from iteration n to iteration $n+1$ and $P^n(x)$ is the direction of descent (i.e. search direction) given by

$$P^n(x) = J'^n(x) + \gamma^n P^{n-1}(x) \tag{10b}$$

which is a conjugation of the gradient direction $J'^n(x)$ at iteration n and the direction of descent $P^{n-1}(x)$ at iteration $n-1$. The conjugate coefficient is determined from

$$\gamma^n = \frac{\int_{x=0}^{L} (J'^n)^2 \, \mathrm{d}x}{\int_{x=0}^{L} (J'^{n-1})^2 \, \mathrm{d}x} \quad \text{with } \gamma^0 = 0. \tag{10c}$$

We note that when $\gamma^n = 0$ for any n, in equation (10b), the direction of descent $P^n(x)$ becomes the gradient direction, i.e. the "steepest descent" method is obtained. The convergence of the above iterative procedure in minimizing the functional J is guaranteed in Ref. [12].

To perform the iterations according to equation (10), we need to compute the step size β^n and the gradient of the functional $J'^n(x)$. In order to develop expressions for the determination of these two quantities, a "sensitivity problem" and an "adjoint problem" are constructed as described below.

5.1. *Sensitivity problem and search step size*

The sensitivity problem is obtained from the original direct problem defined by equation (1) in the following manner. It is assumed that when $f(x)$ undergoes a variation $\Delta f(x)$, $T(x, t)$ is perturbed by $T + \Delta T$. Then replacing in the direct problem f by $f + \Delta f$ and T by $T + \Delta T$, subtracting from the resulting expressions the direct problem and neglecting the second-order terms, the following sensitivity problem for the sensitivity function ΔT is obtained:

$$\frac{\partial^2 \Delta T}{\partial x^2} + \frac{\partial^2 \Delta T}{\partial y^2} = 0 \quad \text{in } \Omega \tag{11a}$$

$$\frac{\partial \Delta T}{\partial x} = 0 \quad \text{at } x = 0 \tag{11b}$$

$$\frac{\partial \Delta T}{\partial x} = 0 \quad \text{at } x = L \tag{11c}$$

$$\frac{\partial \Delta T}{\partial y} = 0 \quad \text{at } y = 0 \tag{11d}$$

$$\Delta T = \Delta f \frac{\partial T}{\partial y} \quad \text{at } y = f(x). \tag{11e}$$

The BEM technique is used to solve this sensitivity problem. The functional $J(\hat{k}^{n+1})$ for iteration $n+1$ is obtained by rewriting equation (5) as

$$J(\hat{f}^{n+1}) = \sum_{i=1}^{m} [T_i(\hat{f}^n - \beta^n P^n) - Y_i]^2 \tag{12a}$$

where we replaced $\hat{f}^{n+1}$ by the expression given by equation (10a). If temperature $T_i(\hat{f}^n - \beta^n P^n)$ is linearized by a Taylor expansion, equation (12a) takes the form

$$J(\hat{f}^{n+1}) = \sum_{i=1}^{m} [T_i(\hat{f}^n) - \beta^n \Delta T_i(P^n) - Y_i]^2 \tag{12b}$$

where $T_i(\hat{f}^n)$ is the solution of the direct problem by using estimate $\hat{f}^n(x)$ for exact $f(x)$ at $x = x_i$. The sensitivity functions $\Delta T_i(P^n)$ are taken as the solutions of problem (11) at the measured positions $x = x_i$ by letting $\Delta f = -P^n$. The search step size β^n is determined by minimizing the functional given by equation (12b) with respect to β^n. The following expression results:

$$\beta^n = \frac{\sum_{i=1}^{m} (T_i - Y_i) \Delta T_i}{\sum_{i=1}^{m} (\Delta T_i)^2}. \tag{13}$$

5.2. *Adjoint problem and gradient equation*

To obtain the adjoint problem, equation (1a) is multiplied by the Lagrange multiplier (or adjoint function) $\lambda(x, y)$ and the resulting expression is inte-

grated over the correspondent space domains. Then the result is added to the right-hand-side of equation (5) to yield the following expression for the functional $J[f(x)]$:

$$J[f(x)] = \int_{x=0}^{L} [T-Y]^2 \delta(x-x_i)\,dx + \int_{x=0}^{L}\int_{y=0}^{f(x)} \lambda\left\{\frac{\partial^2 T}{\partial x^2}+\frac{\partial^2 T}{\partial y^2}\right\}dy\,dx. \quad (14)$$

The variation ΔJ is obtained by perturbing f by Δf and T by ΔT in equation (14), subtracting from the resulting expression the original equation (14) and neglecting the second-order terms. We thus find

$$\Delta J = \int_{x=0}^{L} 2(T-Y)\,\Delta T\,\delta(x-x_i)\,dx + \int_{x=0}^{L}\int_{y=0}^{f(x)} \lambda\left[\frac{\partial^2 \Delta T}{\partial x^2}+\frac{\partial^2 \Delta T}{\partial y^2}\right]dy\,dx \quad (15)$$

where $\delta(x-x_i)$ is the Dirac delta function and x_i, $i = 1$–m, refer to the measured positions. In equation (15), the double integral term is integrated by parts; the boundary conditions of the sensitivity problem given by equations (11(b–e)) are utilized and then ΔJ is allowed to go to zero. The vanishing of the integrands containing ΔT leads to the following adjoint problem for the determination of $\lambda(x)$:

$$\frac{\partial^2 \lambda}{\partial x^2}+\frac{\partial^2 \lambda}{\partial y^2} = 0 \quad \text{in } \Omega \quad (16a)$$

$$\frac{\partial \lambda}{\partial x} = 0 \quad \text{at } x = 0 \quad (16b)$$

$$\frac{\partial \lambda}{\partial x} = 0 \quad \text{at } x = L \quad (16c)$$

$$\frac{\partial \lambda}{\partial y} = -2(T-Y)\delta(x-x_i) \quad \text{at } y = 0 \quad (16d)$$

$$\lambda = 0 \quad \text{at } y = f(x). \quad (16e)$$

The standard techniques of BEM can be used to solve the above adjoint problem.

Finally, the following integral term is left

$$\Delta J = \int_0^L -\left[\frac{\partial \lambda}{\partial y}\frac{\partial T}{\partial y}\right]_{y=f(x)} \Delta f(x)\,dx. \quad (17a)$$

From definition [1], the functional increment can be presented as

$$\Delta J = \int_0^L J'(x)\,\Delta f(x)\,dx. \quad (17b)$$

A comparison of equations (17a, b) leads to the following expression for the gradient of functional $J'(x)$ of the functional $J[f(x)]$:

$$J'(x) = -\left.\frac{\partial \lambda}{\partial y}\frac{\partial T}{\partial y}\right|_{y=f(x)}. \quad (18)$$

5.3. *Computational procedure*

The computational procedure for the solution of this inverse problem using conjugate gradient methods may be summarized as follows: Suppose $\hat{f}^n(x)$ is available at iteration n.

Step 1. Solve the direct problem given by equation (1) for $T(x, t)$.

Step 2. Examine the stopping criterion given by equation (9a) with ε given by equation (9c). Continue if not satisfied.

Step 3. Solve the adjoint problem given by equation (16) for $\lambda(x)$.

Step 4. Compute the gradient of the functional J' from equation (18).

Step 5. Compute the conjugate coefficient γ^n and direction of descent P^n from equations (10c, b), respectively.

Step 6. Set $\Delta f(x) = -P^n(x)$ and solve the sensitivity problem given by equation (11) for $\Delta T(x)$.

Step 7. Compute the search step size β^n from equation (13).

Step 8. Compute the new estimation for $\hat{f}^n(x)$ from equation (10a) and return to step 1.

6. RESULTS AND DISCUSSIONS

To illustrate the validity of the present inverse algorithms in identifying irregular boundary configuration $f(x)$ from the knowledge of temperature recordings, we consider three specific examples where the boundary geometry at $y = f(x)$ are assumed as a sinusoidal, triangular and step function, respectively.

The objective of this article is to show the accuracy of the present approaches in estimating $f(x)$ with no prior information on the functional form of the unknown quantities, which is the so-called function estimation. Moreover, it can be shown numerically that the number of sensors can be reduced when the conjugate gradient method is applied.

In order to compare the results for situations involving random measurement errors, we assume normally distributed uncorrelated errors with zero mean and constant standard deviation. The simulated inexact measurement data $\mathbf{Y}$ can be expressed as

$$\mathbf{Y} = \mathbf{Y}_{\text{exact}} + \omega\sigma \quad (19)$$

where $\mathbf{Y}_{\text{exact}}$ is the solution of the direct problem with an exact $f(x)$; σ is the standard deviation of the measurements; and ω is a random variable that is generated by subroutine DRNNOR of the IMSL [13] and will be within $-2.576 \sim 2.576$ for a 99% confidence bound.

One of the advantages of using the conjugate gradient method is that it does not require a very accurate initial guess of the unknown quantities; this can also be proved when compared with the L–MM in the

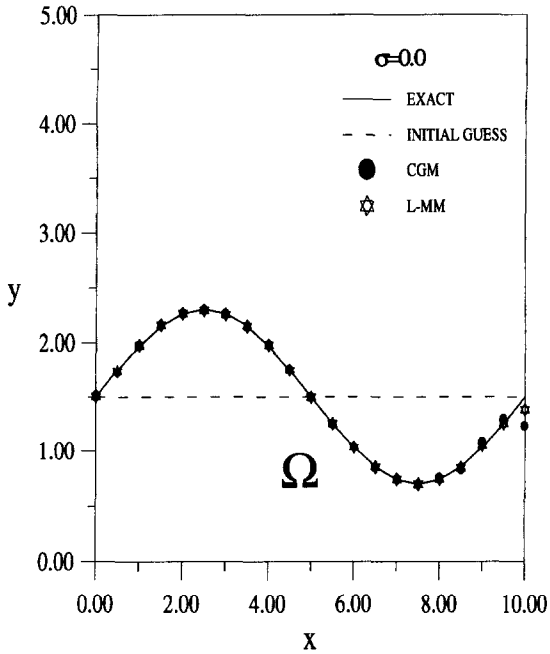

Fig. 2. Inverse solutions by CGM and L–MM with accurate initial guess of $f(x)$ when using $\sigma = 0.0$ and $m = 21$ in case 1.

numerical experiments. In all the test cases considered here we have chosen $L = 10$, $T_0 = 100$, $q_0 = 20$ and 20 linear elements are used on both upper and lower boundaries, while three linear elements are adopted for right and left boundaries. The sensor's locations are always along $y = 0$, i.e. on the lower boundary. We now present below three numerical experiments in determining $f(x)$ by the inverse analysis:

Numerical test case 1. The unknown boundary configuration at $y = f(x)$ is assumed to vary with x in the form

$$f(x) = 1.5 + 0.8 \sin\left(\frac{\pi x}{5}\right); \quad 0 \leqslant x \leqslant L. \qquad (20)$$

The inverse analysis is first performed by using 21 thermocouple measurements (referring to Fig. 1 where the solid triangular dot denotes the sensor's location) with thermocouple spacing $\Delta x = 0.5$. When assuming exact measurements ($\sigma = 0.0$) and using good initial guess $\mathbf{f}^0 = 1.5$, the estimated function of $f(x)$ by using both CGM and L–MM is shown in Fig. 2 for the same convergent criteria $\varepsilon = 0.001$. It can be seen from this figure that both schemes obtained good estimation of $f(x)$ and the CPU time (on 586-60 MHz PC) used in the CGM is about the same as that for the L–MM. This shows that when an accurate initial guess $\mathbf{f}^0$ is provided, the validity of the CGM is about the same as that of the L–MM. Table 1 shows some convergent parameters for the inverse calculation considered here, i.e. initial guess $\mathbf{f}^0$, stopping criteria ε, the number of iterations, CPU time on 586-60 MHz personal computer and average error, respectively. One should note that even though the number of iterations for the L–MM and CGM are 4 and 30, respectively, the CPU time used is about the same. This is because for the L–MM, in each iteration we need to compute the direct problem $(k+1)$ times (when obtaining the Jacobian matrix); however, only three approximate weight of computations (i.e. the direct, sensitivity and adjoint problems) are needed for the CGM. This implies that when the number of unknown parameters k are increased, the CPU time needed for the L–MM will also be increased greatly.

Next, let us see what will happen when the initial guess $\mathbf{f}^0$ is deviated from the exact solutions. The computational situations are the same as the previous one except that the initial guess is now chosen as $\mathbf{f}^0 = 2.5$. The inverse solutions with stopping criteria $\varepsilon = 0.04$ is shown in Fig. 3. It is clear from Fig. 3 that the estimated $f(x)$ is still very accurate for the CGM, but the inverse solutions become poor for the L–MM especially near $x = L$; moreover, the CPU time used for the CGM is also shorter than that for the L–MM. This implies that the CGM is less sensitive to the initial guesses.

The above test cases seem unrealistic, since too many sensors were used in the numerical experiments. Now the question arises, can the number of sensors be reduced with the present approaches?

Let us first take a look at the L–MM. From equation (6) it is obvious that the number of sensors m should be equal to or greater than the number of unknown parameters $(k+1)$, otherwise an indeterminate system of equations is obtained. Therefore, it is impossible to reduce the number of sensor when the L–MM is applied.

However, in the CGM, the measurement temperatures at sensor's locations represent a boundary point heat flux that appeared in the adjoint equation (16). Then it is possible to reduce the number of boundary point heat fluxes even though it will influence the value of J. Now the question is that will this strategy influence the accuracy of the inverse solutions? To answer this, the numerical experiment is proceeded to the next case with $\mathbf{f}^0 = 2.5$, i.e. using $m = 21$ ($\Delta x = 0.5$) and $m = 11$ ($\Delta x = 1.0$), respectively, in estimating $f(x)$ with measurement error $\sigma = 1.0$.

The inverse solutions in predicting $f(x)$ under such an assumption using the CGM is shown in Fig. 4. The average relative error between exact and estimated values are 7.18 and 8.33% for $m = 21$ and $m = 11$, respectively, where the average relative error is defined as

$$\sum_{j=0}^{k} \left| \frac{f(x_j) - \hat{f}(x_j)}{f(x_j)} \right| \div [k+1] \times 100\% \qquad (21)$$

here $(k+1)$ represents the total discrete number of unknown parameters, while f and $\hat{f}$ denote the exact and estimated values of boundary configuration.

From the above comparisons of numerical data we learned that the inverse solutions in predicting $f(x)$

Table 1. The convergent parameters for the inverse calculations

		Initial guess, f^0	Stopping criteria, ε	Number of iteration	CPU time, s	Average error, %
Fig. 2 ($\sigma = 0.0$)	CGM	1.5	0.001	30	65	1.76
	L–MM	1.5	0.001	4	62	0.717
Fig. 3 ($\sigma = 0.0$)	CGM	2.5	0.04	23	51	2.18
	L–MM	2.5	0.04	8	112	6.74
Fig. 4 ($\sigma = 1.0$)	$m = 21$	2.5	21.0	6	13	7.18
	$m = 11$	2.5	11.0	5	12	8.33
Fig. 5 ($\sigma = 0.0$)	$m = 21$	3.5	0.1	10	22	2.65
	$m = 11$	3.5	0.1	8	20	2.67
Fig. 6 ($\sigma = 2.0$)	$m = 21$	3.5	84.0	5	11	3.03
	$m = 11$	3.5	44.0	5	13	3.75
Fig. 7 ($\sigma = 0.0$)	$m = 21$	3.5	0.5	25	54	5.56
	$m = 11$	3.5	0.5	27	56	5.94
Fig. 8 ($\sigma = 2.0$)	$m = 21$	3.5	84.0	5	11	8.65
	$m = 11$	3.5	44.0	4	9	9.72

with 21 sensors are slightly better than that with 11 sensors; however, the latter case is already good enough to be accepted as the inverse solutions. This represents that the number of sensors can be reduced when the CGM is applied.

Besides, when $\sigma = 1.0$, it represents about 2% measurement error since the average measured temperature is about 50. By using this 2% error the resultant average error of the inverse solutions is about 7%; this implies that the CGM is not sensitive to the measurement errors since the measurement errors did not amplify the errors of estimated boundary shape (the errors are in the same order). Therefore, the present technique provides a confident estimate. Only the CGM is used for the rest of the numerical experiments since it is obviously better than L–MM.

Numerical test case 2. In the second test case, $f(x)$ is taken as

$$f(x) = \begin{cases} 1.5+0.3x; & 0 \leqslant x \leqslant \dfrac{L}{2} \\ 4.5-0.3x; & \dfrac{L}{2} \leqslant x \leqslant L \end{cases} \tag{22}$$

where the initial guess for this test case is chosen as $f^0 = 3.5$. The estimation of $f(x)$ by using 21 and 11 sensors with exact measurements $\sigma = 0.0$ shows that for both cases a very good agreement between the estimated and the exact values of $f(x)$ are obtained. The result is shown in Fig. 5.

Next, when 21 and 11 sensors are used and the measurement errors with $\sigma = 2.0$ are considered, the estimations for $f(x)$ are sketched in Fig. 6. When

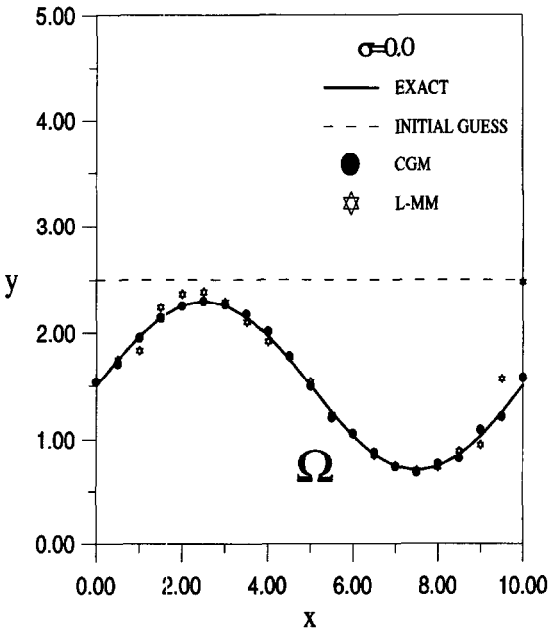

Fig. 3. Inverse solutions by CGM and L–MM with inaccurate initial guess of $f(x)$ when using $\sigma = 0.0$ and $m = 21$ in case 1.

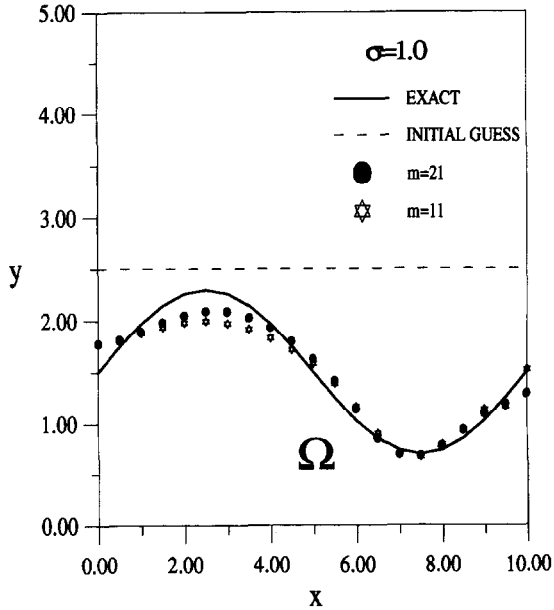

Fig. 4. Inverse solutions by CGM ($\sigma = 1.0$) when using $m = 21$ and $m = 11$ in case 1.

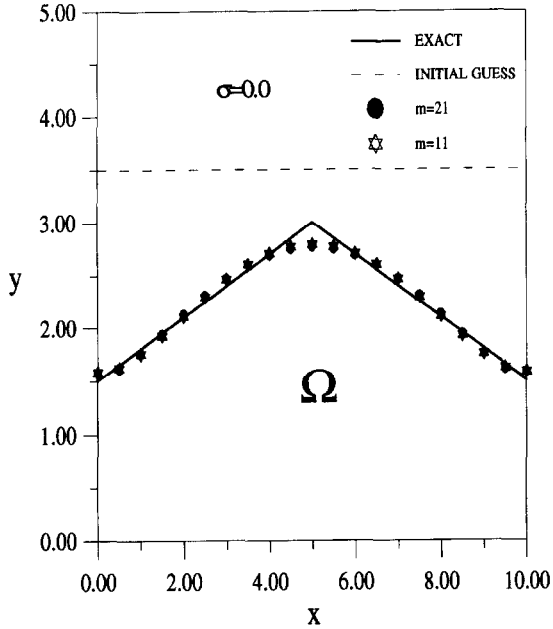

Fig. 5. Inverse solutions by CGM ($\sigma = 0.0$) when using $m = 21$ and $m = 11$ in case 2.

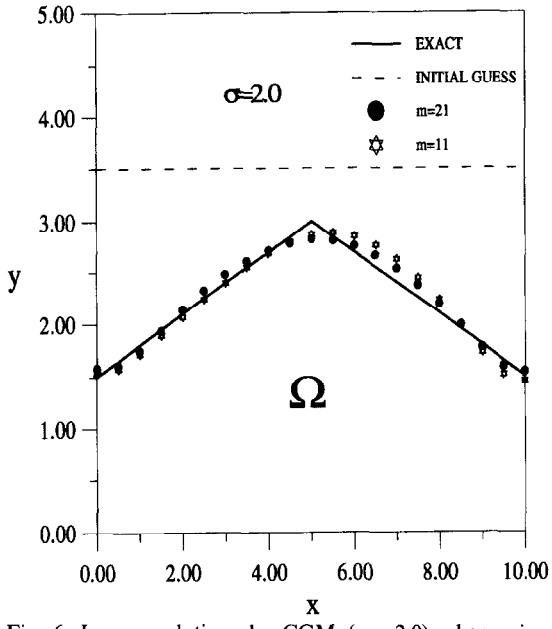

Fig. 6. Inverse solutions by CGM ($\sigma = 2.0$) when using $m = 21$ and $m = 11$ in case 2.

$\sigma = 2.0$, it denotes about 5% measurement error since the average measured temperature is about 35. The resultant average error of the inverse solutions using this error is about 4%. Again, this implies that the CGM is not sensitive to the measurement errors. Table 1 shows some convergent parameters for the inverse calculations of test case 2.

Numerical test case 3. In the third test case, a more strict $f(x)$ is taken as a step function, i.e.

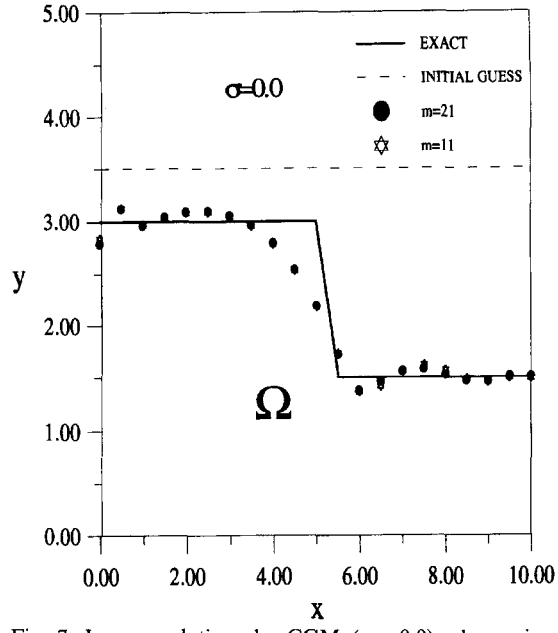

Fig. 7. Inverse solutions by CGM ($\sigma = 0.0$) when using $m = 21$ and $m = 11$ in case 3.

$$f(x) = \begin{cases} 3.0; & 0 \leqslant x < \dfrac{L}{2} \\ 1.5; & \dfrac{L}{2} \leqslant x \leqslant L \end{cases} \tag{23}$$

where the initial guess for this test case is chosen as $f^0 = 3.5$. The estimation of $f(x)$ by using 21 and 11 sensors with exact measurements $\sigma = 0.0$ is shown in Fig. 7. The estimated boundary shape is not so accurate near the discontinuity region.

Next, when 21 and 11 sensors are used and the measurement errors with $\sigma = 2.0$ are considered, the estimations for $f(x)$ are sketched in Fig. 8. When $\sigma = 2.0$, it denotes about 5% measurement error since the average measured temperature is about 35. The resultant average error of the inverse solutions using this error is about 9%. This denotes that the CGM is not sensitive to the measurement errors. Table 1 denotes some convergent parameters for the inverse calculations of test case 3.

From the above numerical test cases 1, 2 and 3, we concluded that the advantages of the CGM in comparison with the L–MM in estimating unknown boundary configurations lie in that: (i) it does not require a very accurate initial guess; (ii) the rate of convergence is fast; and (iii) the number of sensors can be reduced while the accurate inverse solutions can still be obtained. The only advantage of L–MM is that its derivation is simpler than that for the CGM.

7. CONCLUSIONS

The conjugate gradient method (CGM) and Levenberg–Marquardt method (L–MM) with boundary element method (BEM) was successfully applied for

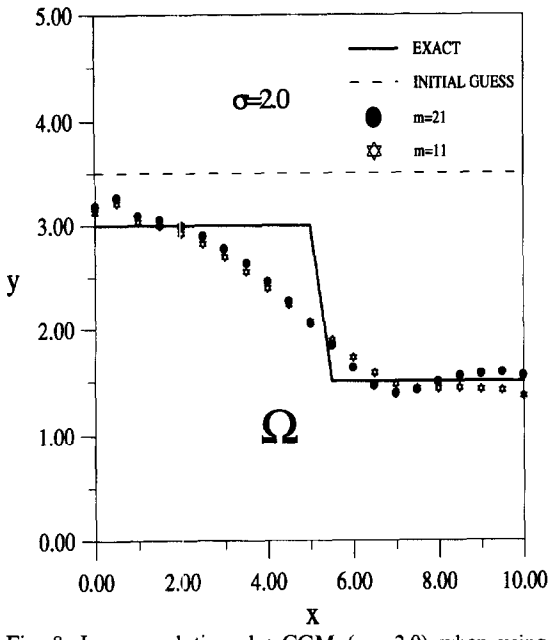

Fig. 8. Inverse solutions by CGM ($\sigma = 2.0$) when using $m = 21$ and $m = 11$ in case 3.

the solution of the inverse problem to determine the unknown irregular boundary configuration by utilizing temperature readings. Several test cases involving different functional forms of $f(x)$ and measurement errors were considered. The results show that the CGM does not require an accurate initial guess of the unknown quantities, needs very short CPU time on 586-60 MHz PC and requires fewer sensors when compared with the L–MM in performing the inverse calculations.

Acknowledgment—This work was supported in part through the National Science Council, Republic of China, Grant number NSC-86-2611-E-006-002.

REFERENCES

1. Alifanov, O. M., Solution of an inverse problem of heat conduction by iteration methods. *Journal of Engineering Physics*, 1972, **26,** 471–476.
2. Huang, C. H. and Ozisik, M. N., Inverse problem of determining unknown wall heat flux in laminar flow through a parallel plate duct. *Numerical Heat Transfer, Part A*, 1992, **21,** 55–70.
3. Huang, C. H. and Yan, J. Y., An inverse problem in simultaneously measuring temperature dependent thermal conductivity and heat capacity. *International Journal of Heat and Mass Transfer*, 1995, **38,** 3433–3441.
4. Terrola, P., A method to determine the thermal conductivity from measured temperature profiles. *International Journal of Heat and Mass Transfer*, 1989, **32,** 1425–1430.
5. Huang, C. H. and Ozisik, M. N., Optimal regularization method to determine the unknown strength of a surface heat source. *International Journal of Heat and Fluid Flow*, 1991, **12,** 173–178.
6. Huang, C. H., Ozisik, M. N. and Sawaf, B., Conjugate gradient method for determining unknown contact conductance during metal casting. *International Journal of Heat and Mass Transfer*, 1992, **35,** 1779–1786.
7. Hsieh, C. K. and Su, K. C., A methodology of predicting cavity geometry based on the scanned surface temperature data-prescribed surface temperature at the cavity side. *Journal of Heat Transfer*, 1980, **102,** 324–329.
8. Das, S. and Mitra, A., An algorithm for the solution of inverse Laplace problems and its application in flaw identification in materials. *Journal of Computational Physics*, 1992, **99,** 99–105.
9. Kassab, A. J. and Pollard, J., A cubic spline anchored grid pattern algorithm for high resolution detection of subsurface cavities by the IR-CAT method. *Numerical Heat Transfer, Part B*, 1994, **26,** 63–78.
10. Marquardt, D. M., An algorithm for least-squares estimation of nonlinear parameters. *Journal of Social Industrial Applied Mathematics*, 1963, **11,** 431–441.
11. Brebbia, C. A. and Dominguez, J., *Boundary Elements, An Introductory Course*. McGraw-Hill, New York, 1989.
12. Lasdon, L. S., Mitter, S. K. and Warren, A. D., The conjugate gradient method for optimal control problem. *IEEE Transactions on Automatic Control*, 1967, **AC-12,** 132–138.
13. IMSL Library Edition 10.0, User's Manual: Math Library Version 1.0, IMSL, Houston, TX, 1987.